

CHAPTER IV

RESULTS AND DISCUSSION

4.1 Preparation of six medicinal plants in Northern Thailand extract

Six kinds of medicinal plant in Northern Thailand were collected from San Pa Thong district, Chiang Mai province, Thailand on May, 2005. The medicinal plants were extracted with 95% ethanol by a continuous technique. Table 3 showed the percentage of yields of ethanol extracts from dried plant material.

Table 3. List of plant species, part used and the percentage yields

Plant	Yield (w/w) (%) ^a	Part used	Extracted color
<i>C. sappan</i>	13.67	Heartwood	Redness brown
<i>L. rubra</i>	12.87	Stem	Black brown
<i>S. albiflorum</i>	8.39	Root	Brown
<i>V. volkamerifolia</i>	5.64	Root	Brown
<i>S. oleosa</i>	6.46	Stem	Redness brown
<i>H. integrifolia</i>	4.76	Stem	Brown

^a Percentage yields from the dried plant material.

4.2 Optimization of *in vitro* antioxidative capacity methods

The antioxidant activity of the plant extracts cannot be evaluated by only a single method due to the complex nature of phytochemicals, a single method due to the complex nature of phytochemicals, so it is important to employ commonly accepted assays to evaluate the antioxidant activity of plant extracts. Various methods have been developed and applied to evaluate the antioxidant capacities. It has to be appreciated

that is no universal method by which antioxidant capacities can be measured accurately and quantitatively. The antioxidants are capable of exerting their effect by different mechanisms and their capacities are determined by many factors. Therefore, great care should be taken in the design of experimental conditions and the interpretation of the data. Besides, the optimal condition for antioxidant capacities assay was carried out to determine. In this experiment, we modified two methods to determination antioxidant capacity, which related to anti-inflammatory property.

4.2.1 Superoxide anion radical scavenging activity assay

This study is a method for the scavenging $O_2^{\bullet-}$ that was generated in a non-enzymatic system using phenazine methosulfate (PMS) and reduced β -nicotinamide adenine dinucleotide (NADH) system by oxidation of NADH and analyzed by the reduction of nitroblue tetrazolium (NBT). The chemicals used in this protocol had scanning absorption wavelength from 200 – 700 nm spectrophotometrically. The absorption spectrums were illustrated on Figure 8-11.

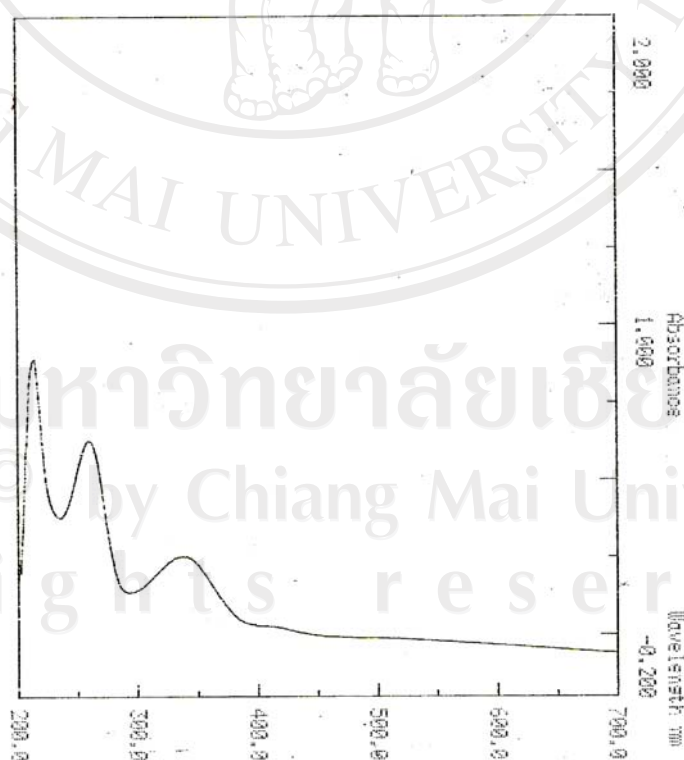


Figure 8. The absorption spectrum of β -nicotinamide adenine dinucleotide (NADH)

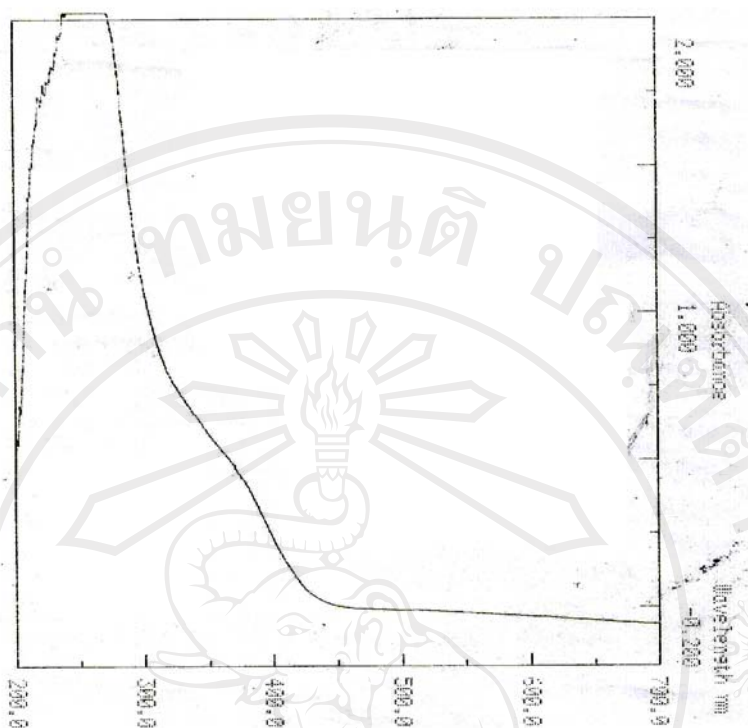


Figure 9. The absorption spectrum of nitroblue tetrazolium (NBT)

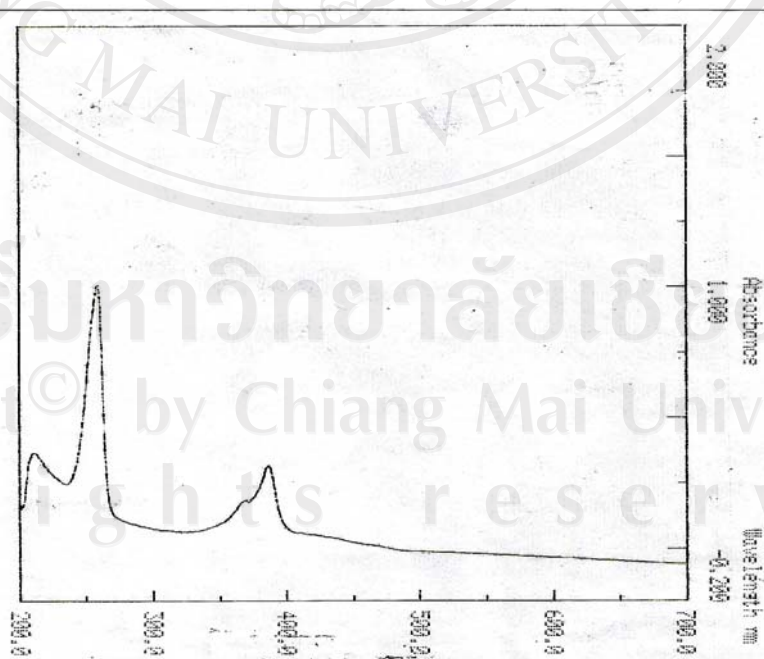


Figure 10. The absorption spectrum of phenazine methosulfate (PMS)

Figure 8, 9, and 10 showed the absorption spectrum of NADH, NBT and PMS, respectively. NADH has the maximum absorption at wavelength 260 and 340 nm. NBT has the maximum absorption at wavelength 260 nm. PMS has the maximum absorption at wavelength 260 and 390 nm. The maximum absorption of the reaction mixture, which containing NADH, NBT, PMS, and EDTA was 560 nm, spectrophotometrically as showed on Figure 11. In summarize, NADH, NBT, and PMS were not interference the maximum absorption of the reaction mixture.

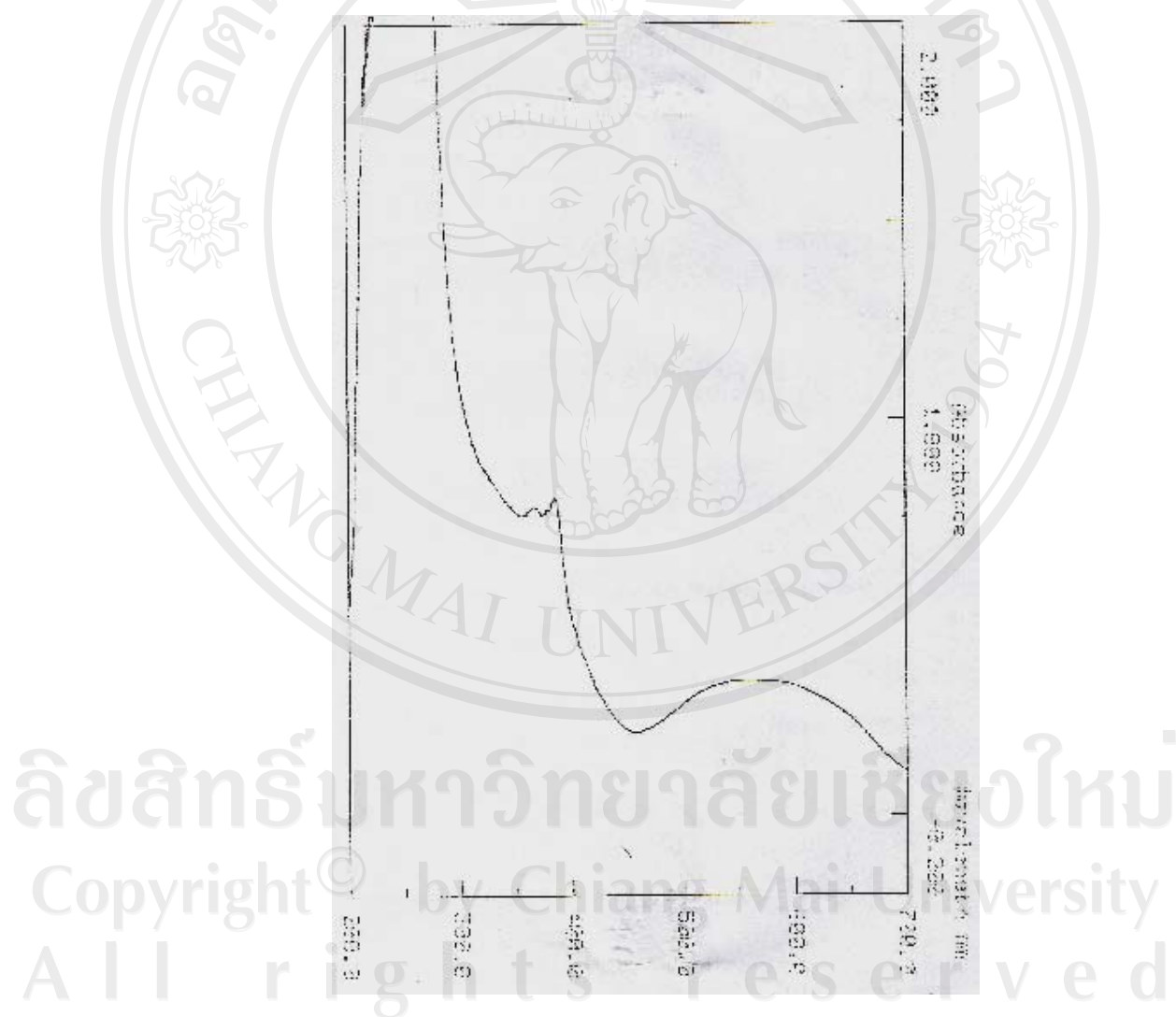


Figure 11. The absorbance spectrum of reaction mixture (NADH, NBT, PMS, and EDTA)

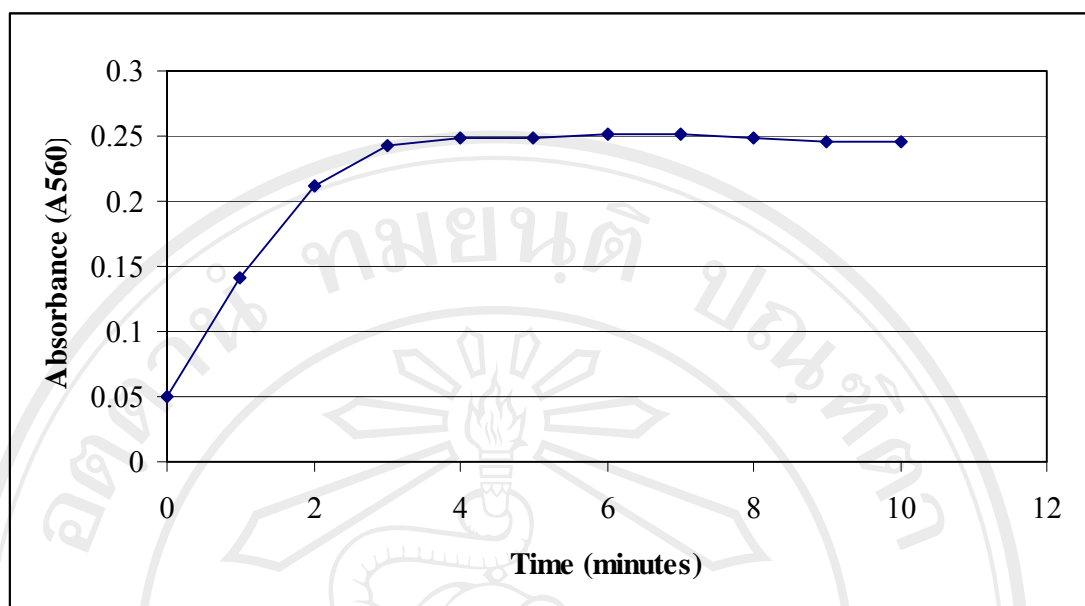


Figure 12. Time-dependent superoxide anion radical production from NADH

Figure 12 exhibited the time-dependent superoxide anion production from NADH, which was oxidized by PMS and analyzed by the reduction of NBT at the maximum absorption 560 nm, spectrophotometrically. The incubation time for NADH to generate a maximum concentration of superoxide anion radical was 5 minutes at room temperature. After 7 minutes incubation, superoxide anion radical was slightly decrease because of superoxide anion radical has a short half-life.

4.2.2 Nitric oxide scavenging activity assay

Sodium nitroprusside in aqueous solution at the physiological pH spontaneously generates NO. It interacts with oxygen to produce a nitrite ion which can be observed using Griess reagent. In this experiment, we observed the maximum absorption wavelength Griess reagent, and reaction mixture (SNP and Griess reagent) as showed in Figure 13 and 14, respectively.

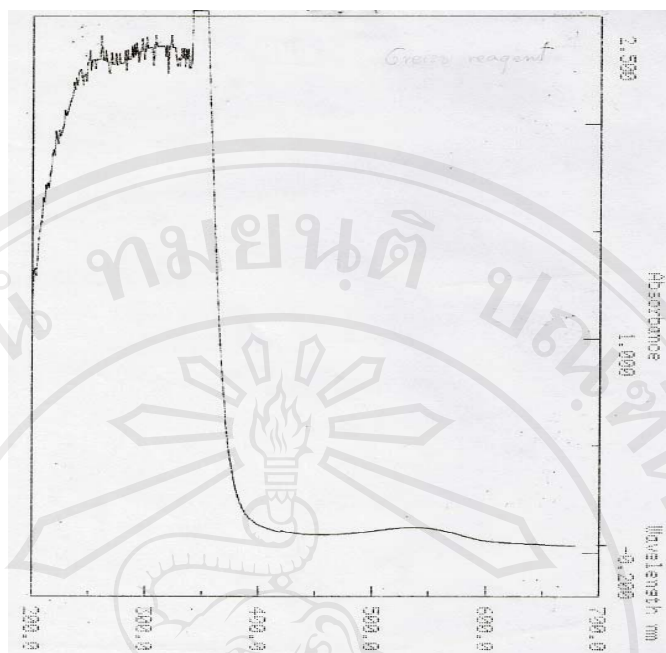


Figure 13. The absorption spectrum of Griess reagent



Figure 14. The absorbance spectrum of reaction mixture (SNP and Griess reagent)

SNP is known to decompose in physiological condition and produce NO, which interacts with oxygen to produce a nitrite ion that can be estimated using Griess reagent. The incubation time for SNP to generate a maximum concentration of nitrite ions are 180 minutes (Figure 15).

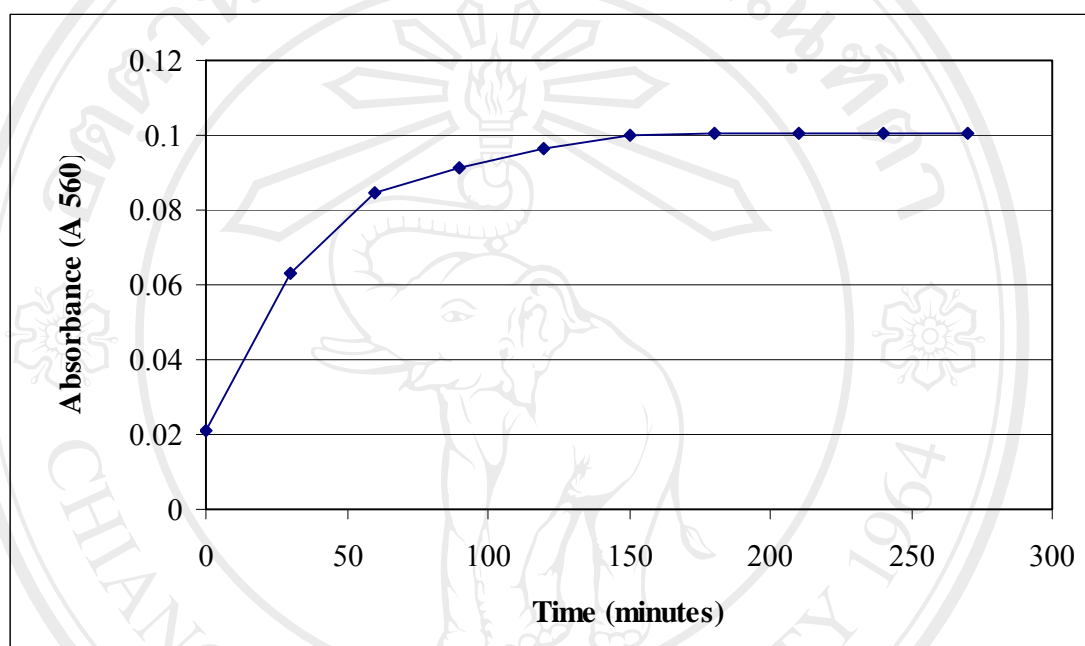


Figure 15. Time-dependent nitric oxide production from sodium nitroprusside

4.3 Optimization of DNA damage protection-induced by Fenton reaction

It is now clear that most of the DNA from animal and bacterial sources is restrained in the cell in a supercoiled or superhelical configuration. Small viral and plasmid DNA can readily be isolated in this supercoiled form (Dabis, 1986). OH^\bullet radicals are generated through Fenton reaction from hydrogen peroxide in the presence of trace amounts of Fe. OH^\bullet can damage DNA via hydrogen transfer from C-H units of the sugar and addition to all the bases, is to analyze their effects on the migratory properties of small supercoiled DNAs in agarose under the influence of an electric field.

4.3.1 Determination of suitable plasmid DNA concentration

Plasmid DNA PUC18 initial concentration of 25-100 ng/ μ l was visualized under a UV transilluminator after electrophoresis, the electrophoresis bands were illustrated in Figure 16.

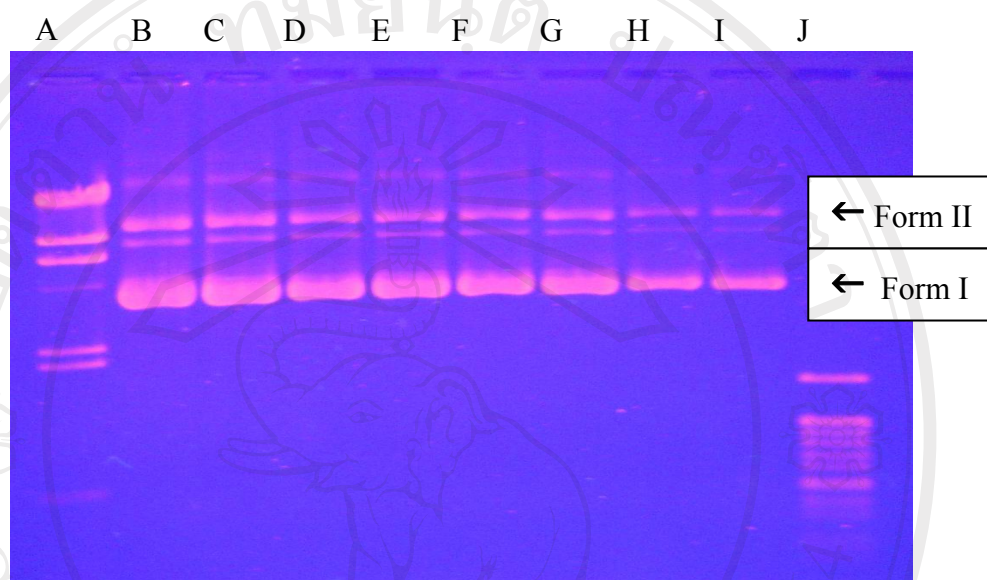


Figure 16. Electrophoresis picture of different concentrations plasmid DNA PUC18. Lanes represent: (A) Lambda Hind III; (B and C) 200 ng/ μ l PUC18; (D and E) 150 ng/ μ l PUC18; (F and G) 100 ng/ μ l PUC18; (H and I) 50 ng/ μ l PUC18; (J) 100 bp ladder; (Form II) DNA relaxed form; (Form I) DNA supercoiled form.

Figure 16 showed the electrophoresis picture of different concentrations plasmid DNA PUC18. At physiological condition, plasmid DNA was composed of mostly supercoiled form (form I) and a small amount of the relaxed form (form II). Plasmid DNA PUC18 at 50 ng/ μ l exhibited sharper bands than another concentrations. The electrophoresis band represented between supercoiled form and relaxed form was linear DNA molecule (form III).

4.3.1 Determination of suitable hydrogen peroxide concentration

This study exhibited a breakage of plasmid DNA PUC18 when Fe(II) or H₂O₂ was added separately into the plasmid DNA PUC18 solution. At a fixed Fe(II) concentration, the addition of increasing amount of H₂O₂ led to increasing plasmid DNA

PUC18 breakage. In this study, the suitable H_2O_2 concentration for determination of plasmid DNA damage induced by Fenton reaction was 25 mM as shown in Figure 17.

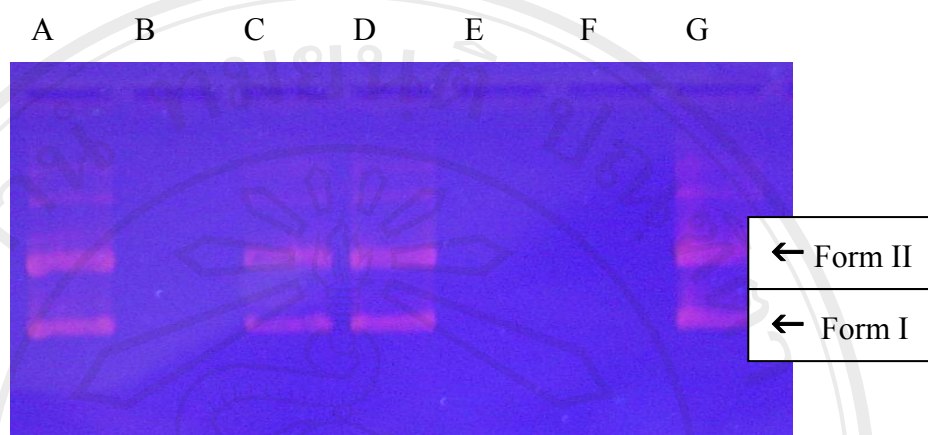


Figure 17. Electrophoresis picture of plasmid DNA PUC18. Lanes represent: (A) $50\mu\text{g}/\mu\text{l}$ PUC18 (no Fe (II) or H_2O_2); (B) $50\mu\text{g}/\mu\text{l}$ PUC18 + 100 mM H_2O_2 + $8\mu\text{M}$ Fe(II) ; (C) $50\mu\text{g}/\mu\text{l}$ + 100 mM H_2O_2 (D) $50\mu\text{g}/\mu\text{l}$ PUC18 + $8\mu\text{M}$ Fe(II); (E) $50\mu\text{g}/\mu\text{l}$ PUC18 + 50 mM H_2O_2 + $8\mu\text{M}$ Fe(II); (F) $50\mu\text{g}/\mu\text{l}$ PUC18 + 25 mM H_2O_2 + $8\mu\text{M}$ Fe(II); (G) $50\mu\text{g}/\mu\text{l}$ PUC18 + 5 mM H_2O_2 + $8\mu\text{M}$ Fe(II)

4.4 Evaluation of antioxidant activity

4.4.1 ABTS free radical cation decolorization assay

In this study, ABTS $^{\bullet+}$ decolorization assay is a method for the scavenging ABTS $^{\bullet+}$. ABTS $^{\bullet+}$ has the maximum adsorption at wavelength 645 nm and 734 nm. In this method, the wavelength 734 nm was used to antioxidant capacity because this wavelength has minimum interference from other components and from sample turbidity. The ABTS $^{\bullet+}$ is a free radical with adsorption band at 734 nm. It loses this adsorption when receiving an electron, which results in a visually noticeable decolorization from blue to clear. Because it can accommodate many sample in a short period and sensitive enough to detect active ingredients at a low concentrations, it has been widely used for screening antiradical activities of fruit and vegetable juices or extracts. The samples were determined for the antioxidant capacity by ABTS $^{\bullet+}$ scavenging method which ABTS $^{\bullet+}$ was generated by using oxidizing agents (potassium persulfate). The antioxidant capacity

was determined by the decolorization of the $\text{ABTS}^{\bullet+}$ (absorbance at 734 nm.). The extent of decolorization is represented as percentage inhibition of the $\text{ABTS}^{\bullet+}$. The unit of the measurement in this assay is the VCEAC and TEAC, which refer to gram of standard (vitamin C, and Trolox) with the equivalent antioxidant capacity to 1 gram of sample. Vitamin C and trolox showed a dose-dependent manner in $\text{ABTS}^{\bullet+}$ scavenging activity. The concentration-response curve and separately prepared stock standard vitamin C and trolox are illustrated in Figure 18 and 19, respectively

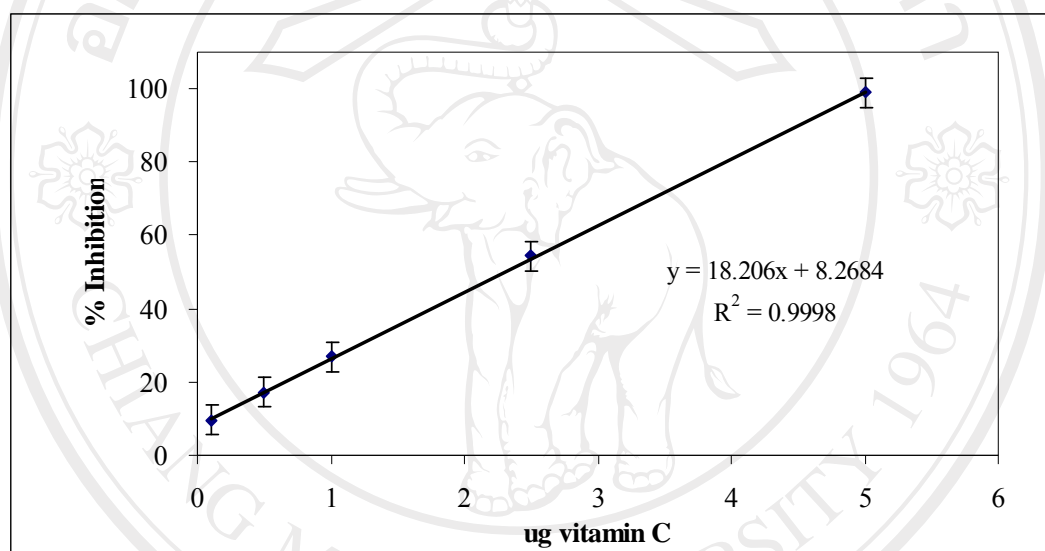


Figure 18. Dose-response curve for the absorbance at 734 nm of $\text{ABTS}^{\bullet+}$ as a function of amount of standard vitamin C ($P < 0.5$)

The percentage inhibition of absorbance at 734 nm was calculated and plotted as a function of concentration of standard vitamin C solution is illustrated in Figure 20. The representative regression coefficient (R^2) was 0.9998 and the linear regression equation was $y=18.206x + 8.2684$. Standard trolox solution was calculated and plotted with the same standard vitamin C solution, which is illustrated in Figure 18. The representative regression coefficient (R^2) was 0.9999 and the linear regression equation was $y=14.859x + 1.1024$.

The ABTS free radical decolorization assay was used to determine antioxidative capacity. The different concentrations of six ethanol extracts were tested $\text{ABTS}^{\bullet+}$ scavenging activity. Antioxidant capacity was reported as VCEAC and TEAC. All of

extracts and reference standard were exhibited the ABTS^{•+} scavenging activity in dose-dependent manner that was statistically significant ($P < 0.05$) The results were shown in Figure 20 and 21, respectively.

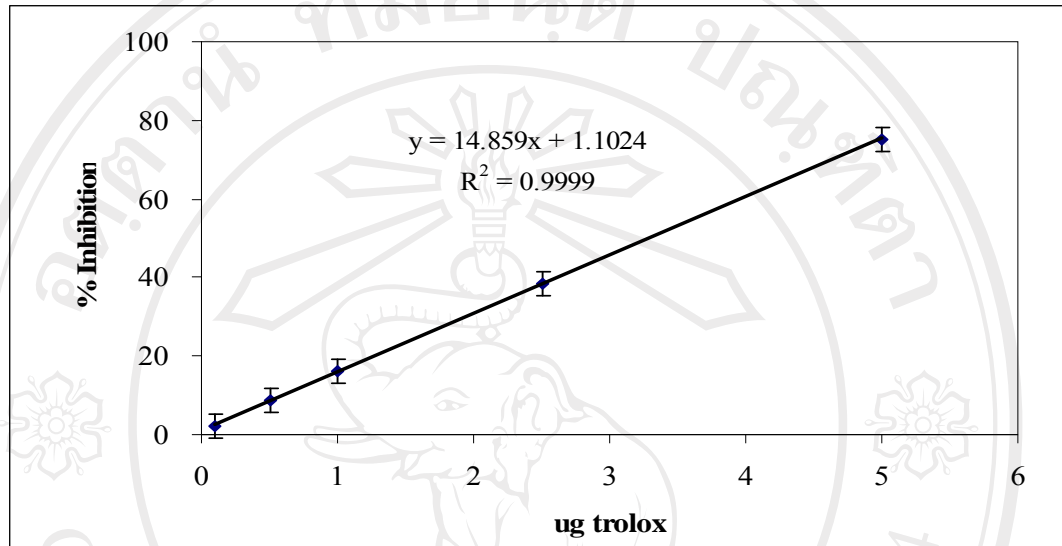


Figure 19. Dose-response curve for the absorbance at 734 nm of ABTS^{•+} as a function of amount of standard trolox ($P < 0.5$)

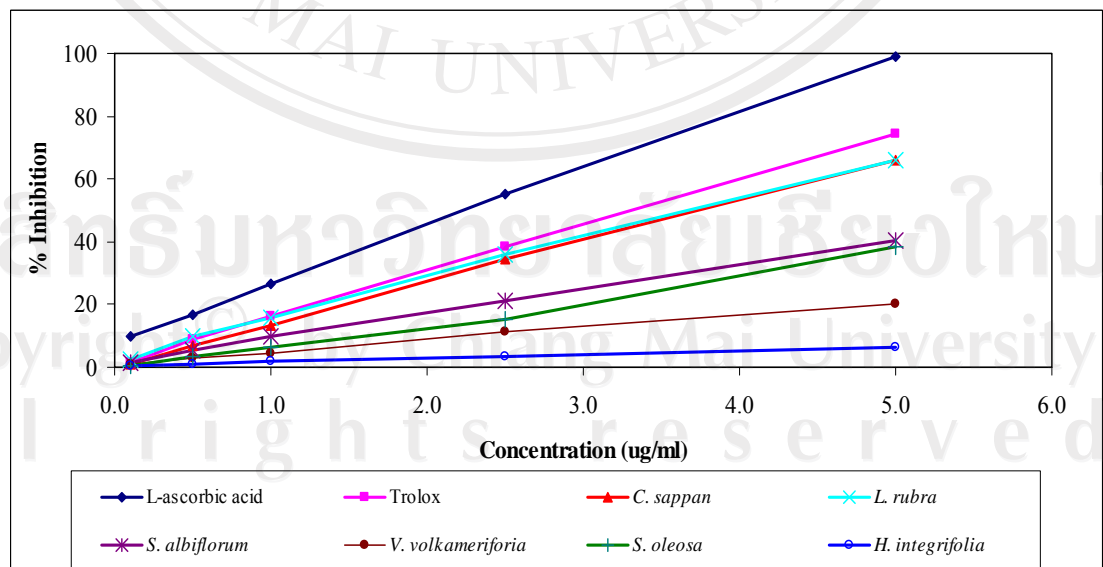


Figure 20. Dose-response curve for ABTS^{•+} scavenging activity of six medicinal plants in Northern Thailand extract

Table 4. VCEAC and TEAC of six medicinal plants in Northern Thailand extract. The data are expressed as the mean \pm SD (n=3). The results are significantly difference at $P < 0.05$

Plant extracts	VCEAC (gram of L-ascorbic acid/ 1 gram of extract)	TEAC (gram of trolox/ 1 gram of extract)
<i>C. sappan</i>	0.5782 \pm 0.0042 ^e	0.9159 \pm 0.0055 ^e
<i>L. rubra</i>	0.6107 \pm 0.0038 ^f	0.9485 \pm 0.0052 ^f
<i>S. albiflorum</i>	0.2834 \pm 0.0033 ^d	0.5592 \pm 0.0049 ^d
<i>V. volkameriforia</i>	0.0598 \pm 0.0028 ^b	0.2854 \pm 0.0049 ^b
<i>S. oleosa</i>	0.1524 \pm 0.0036 ^c	0.3872 \pm 0.0057 ^c
<i>H. integrifolia</i>	0.0105 \pm 0.0009 ^a	0.0583 \pm 0.0029 ^a

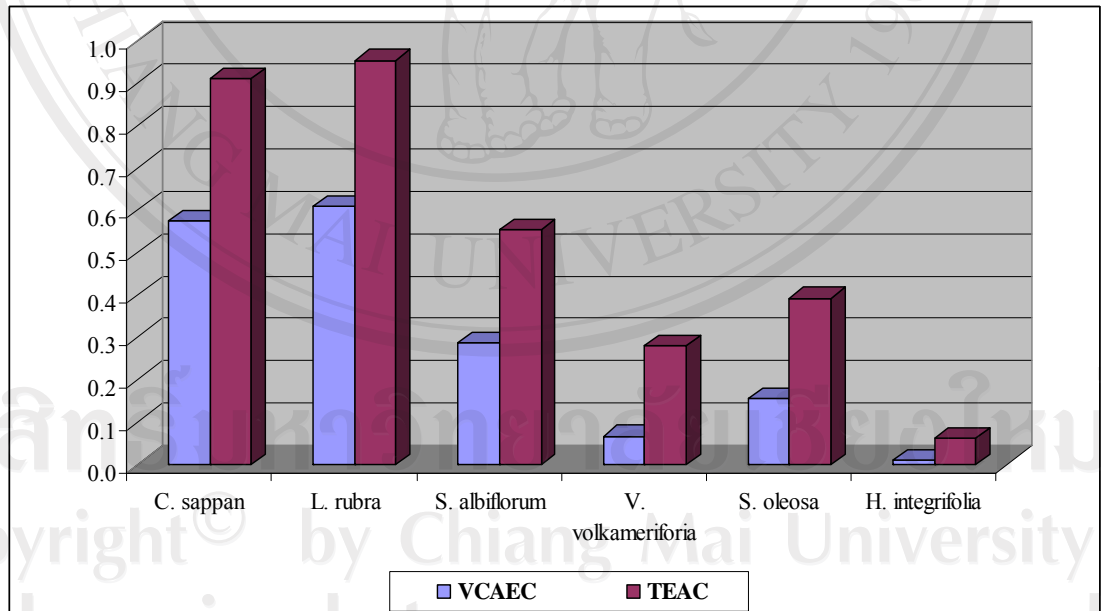


Figure 21. VCEAC and TEAC of six medicinal plants in Northern Thailand extract

Figure 21 exhibited the Vitamin C Equivalent Antioxidant Capacity (VCEAC) of *C. sappan*, *L. rubra*, *S. albiflorum*, *V. volkameriforia*, *S. oleosa*, and *H. integrifolia*. ABTS cation radical scavenging activity of those samples followed the following order:

L. rubra > *C. sappan* > *S. albiflorum* > *S. oleosa* > *V. volkamerifolia* > *H. integrifolia*. *L. rubra* showed the strongest ABTS^{•+} scavenging activity.

4.4.2 Superoxide anion radical scavenging activity assay

Reactive oxygen species, such as superoxide anion radical is known to play in wide variety of pathological manifestations in almost every animal species. The assay was based on the capacity of the ethanolic extracts to inhibit formazan formation by scavenging the superoxide anion radicals generated in NADH-PMS system. The decrease of absorbance at 560 nm with antioxidants (tested sample) thus indicates the consumption of superoxide anion radicals in the reaction mixture.

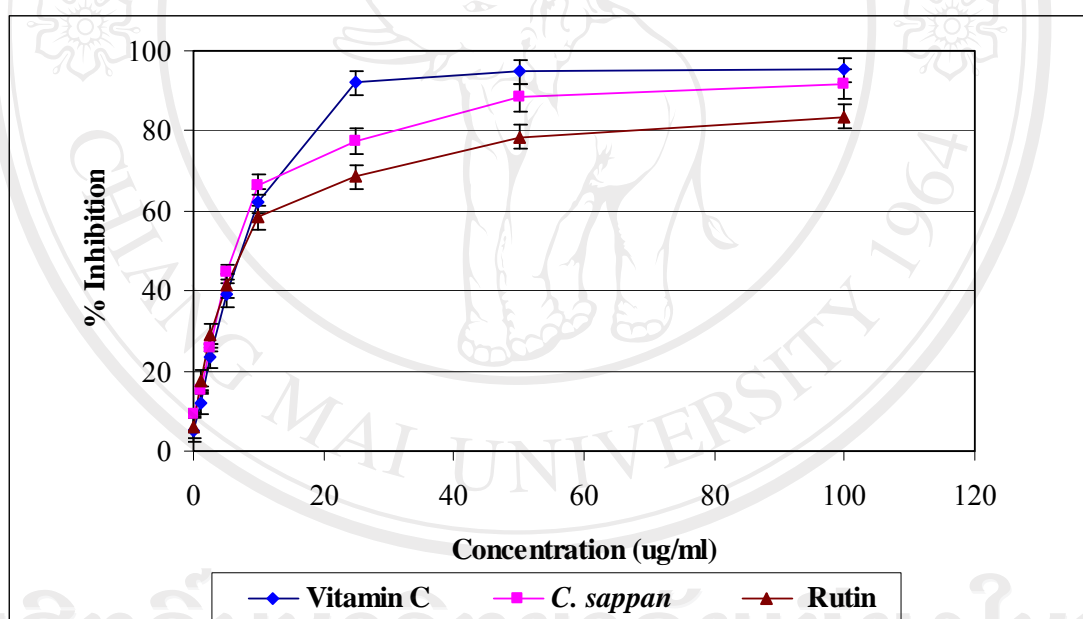


Figure 22. Dose-response curve for superoxide anion radical scavenging activity of *C. sappan*

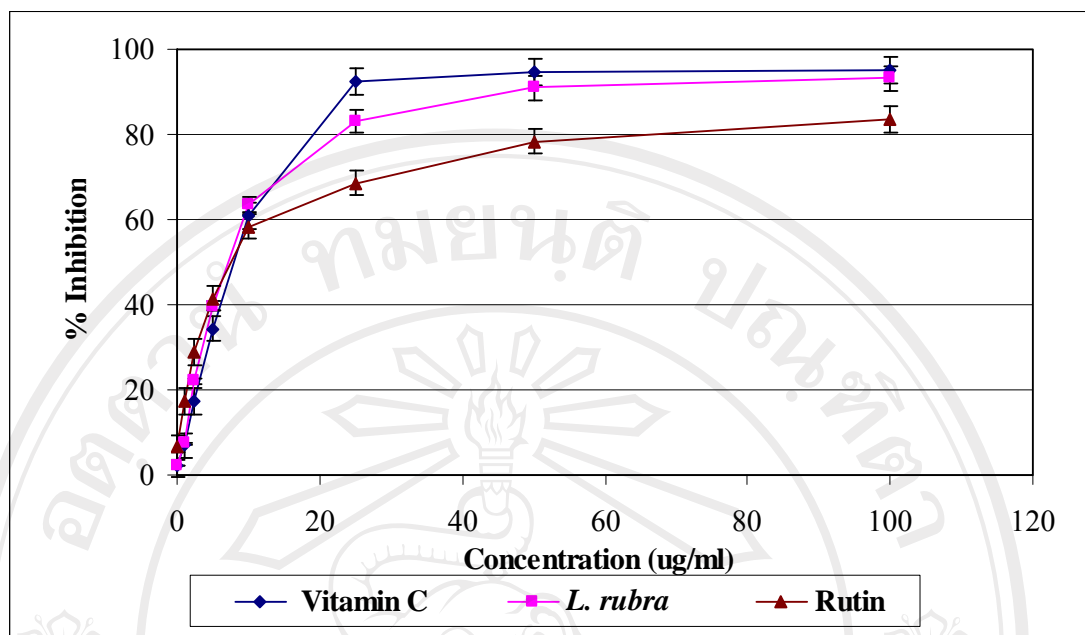


Figure 23. Dose-response curve for superoxide anion radical scavenging activity of *L. rubra*

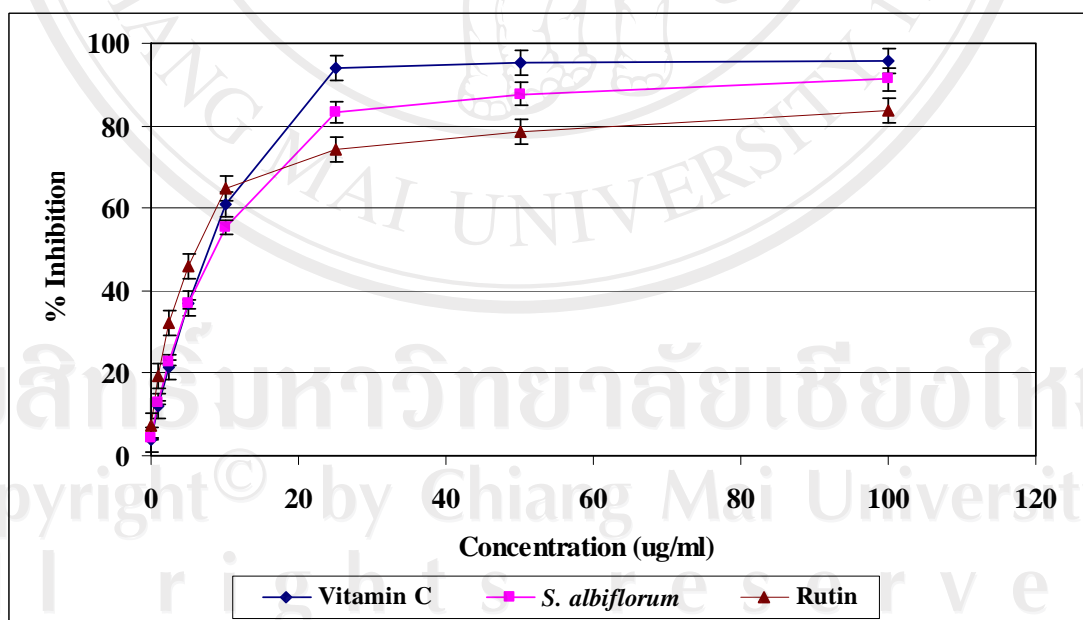


Figure 24. Dose-response curve for superoxide anion radical scavenging activity of *S. albiflorum*

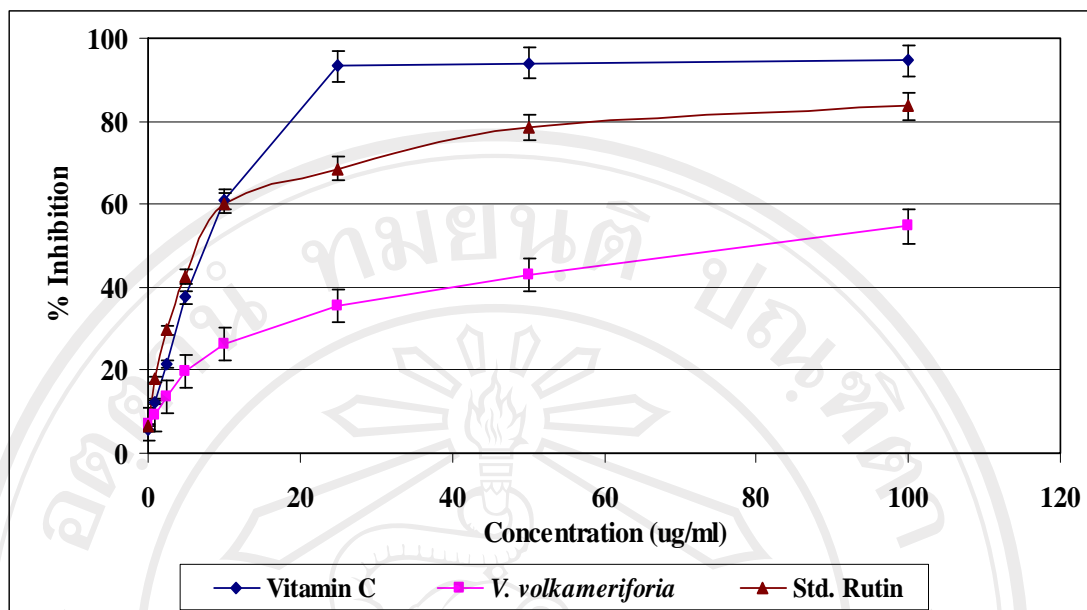


Figure 25. Dose-response curve for superoxide anion radical scavenging activity of *V. volkamerifolia*

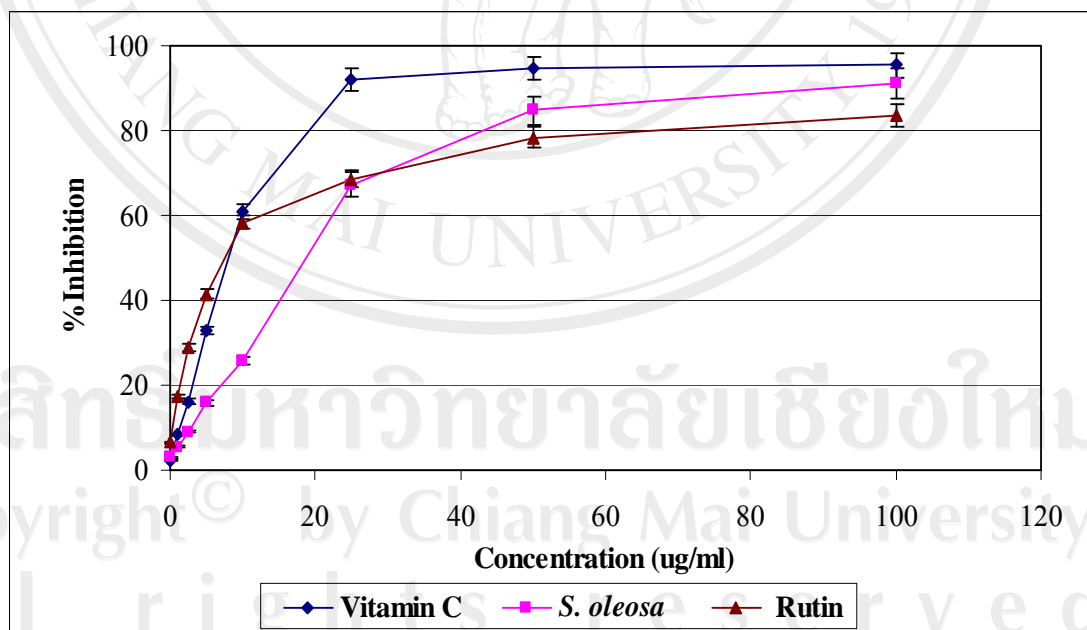


Figure 26. Dose-response curve for superoxide anion radical scavenging activity of *S. oleosa*

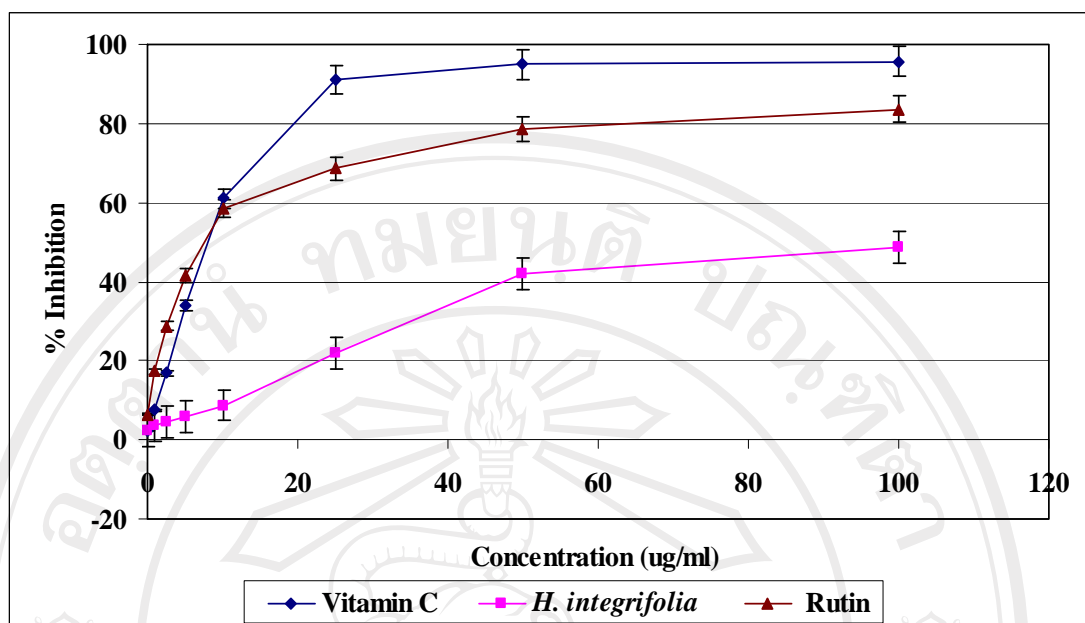


Figure 27. Dose-response curve for superoxide anion radical scavenging activity of *H. integrifolia*

Table 5. 50% Effective concentration of six medicinal plants in Northern Thailand extract on superoxide anion radical scavenging activity. The data are expressed as the mean \pm SD (n=3). The results are significantly difference at $P < 0.05$.

Plant extracts	Standard	Superoxide anion radical scavenging activity
		EC ₅₀ (μ g/ml)
<i>C. sappan</i>	-	7.73 \pm 0.06 ^b
<i>L. rubra</i>	-	9.27 \pm 0.09 ^d
<i>S. albiflorum</i>	-	8.46 \pm 0.08 ^c
<i>V. volkamerifolia</i>	-	12.60 \pm 0.26 ^e
<i>S. oleosa</i>	-	17.45 \pm 0.44 ^f
<i>H. integrifolia</i>	-	28.32 \pm 0.56 ^g
-	L- ascorbic acid	6.65 \pm 0.07 ^a
-	Rutin	7.83 \pm 0.13 ^b

Figure 22-27 exhibited the dose-response curve for the superoxide anion radicals scavenging activity of different concentrations of *C. sappan*, *L. rubra*, *S. albiflorum*, *V. volkamerifolia*, *S. oleosa* and *H. integrifolia*, respectively, by the PMS-NADH superoxide anion generating system. Apparently, the scavenging effect on the superoxide anion radical also increasing with extracts concentration to a certain extent and then leveled off with further increase in extracts concentration. Vitamin C (L-ascorbic acid), used as a positive control, showed the highest superoxide anion scavenging activity. The results were found statistically significant ($P < 0.05$). The 50% effective concentration (EC_{50}) was calculated according the relationship of concentration and %inhibition.

EC_{50} of *C. sappan*, *L. rubra*, *S. albiflorum*, *V. volkamerifolia*, *S. oleosa*, *H. integrifolia*, L-ascorbic acid, and rutin was showed in Table 5. Superoxide anion scavenging activity of those samples followed the following order: L-ascorbic acid > *C. sappan* > rutin > *S. albiflorum* > *L. rubra* > *V. volkamerifolia* > *S. oleosa* > *H. integrifolia*. *C. sappan* exhibited the highest superoxide anion radical scavenging activity. The activity of these extract was less than L-ascorbic acid but better than rutin, which used as the positive control.

4.4.3 Nitric oxide radical scavenging activity assay

When dissolved SNP in the physiological solution, it will release nitric oxide. Therefore, an SNP solution in the presence of various extracts with Griess reagent can be used to evaluate the nitric oxide scavenging effect of extracts.

In this study, curcumin was used as the reference NO radical scavenger. All tested compounds inhibited nitrite formation by competing with oxygen atom to react with NO. This leads to the reduction of nitrite concentration in the reaction mixture.

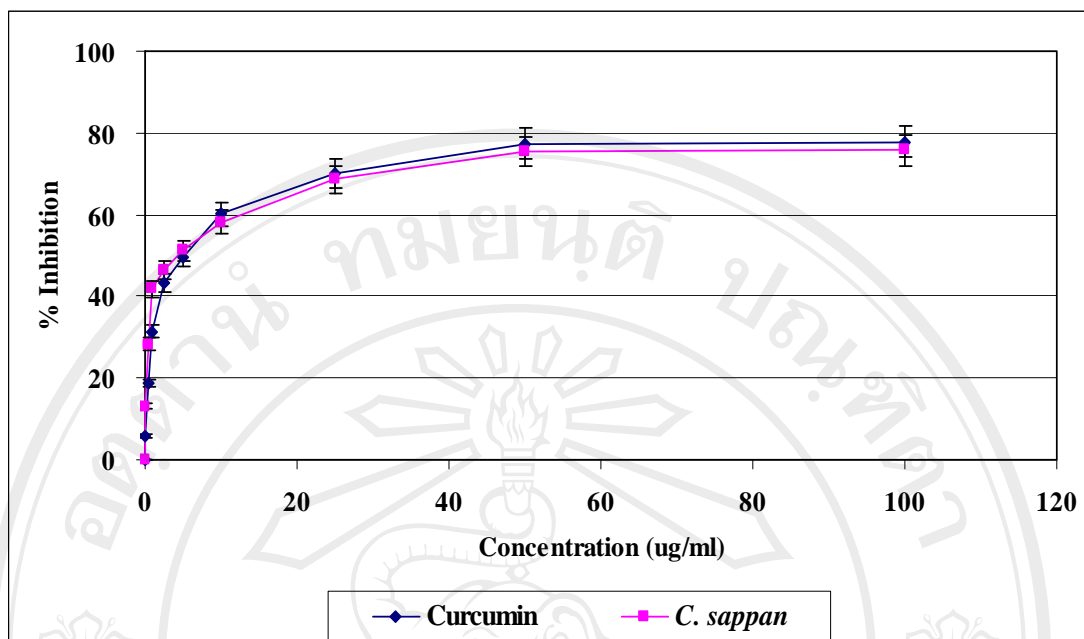


Figure 28. Dose-response curve on nitric oxide scavenging activity of *C. sappan*

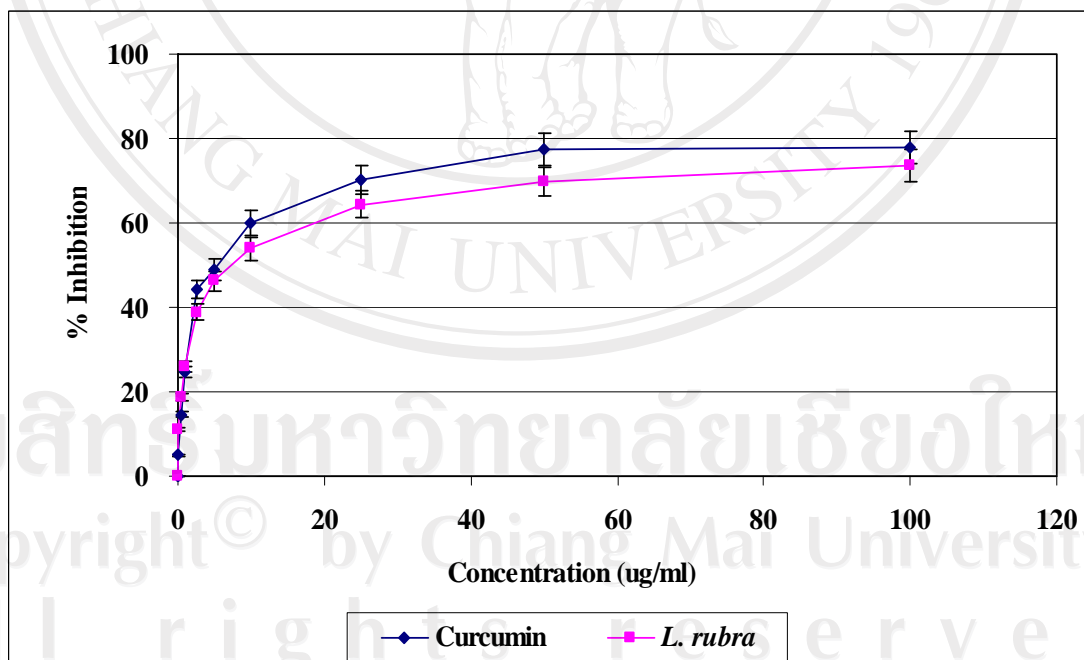


Figure 29. Dose-response curve on nitric oxide scavenging activity of *L. rubra*

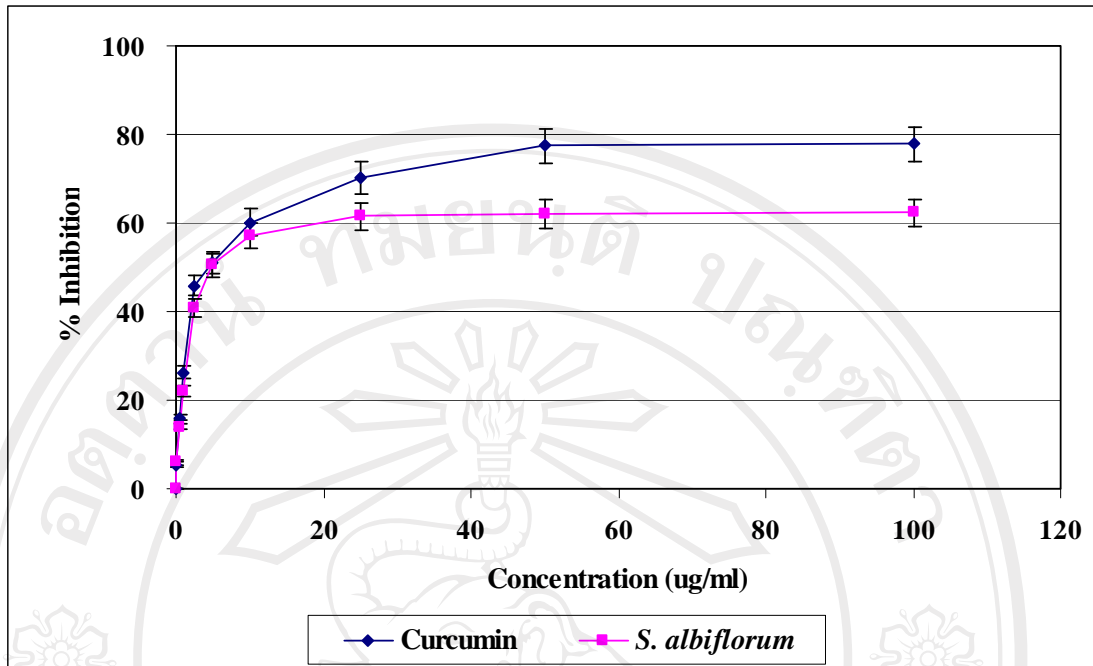


Figure 30. Dose-response curve on nitric oxide scavenging activity of *S. albiflorum*

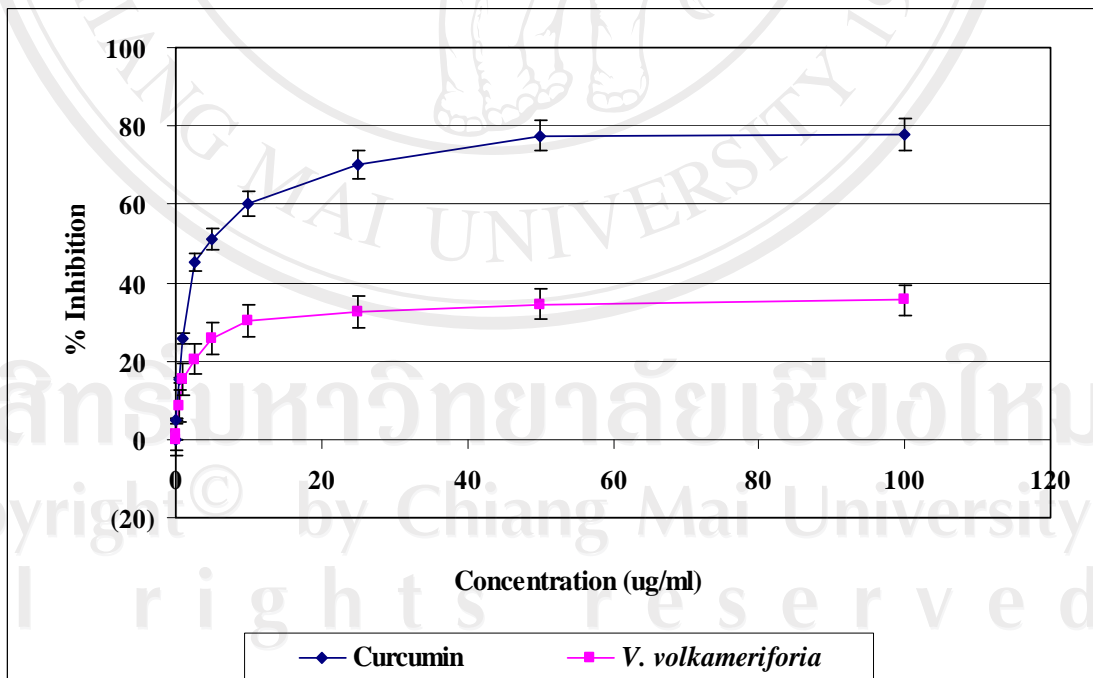


Figure 31. Dose-response curve on nitric oxide scavenging activity of *V. volkamerifolia*

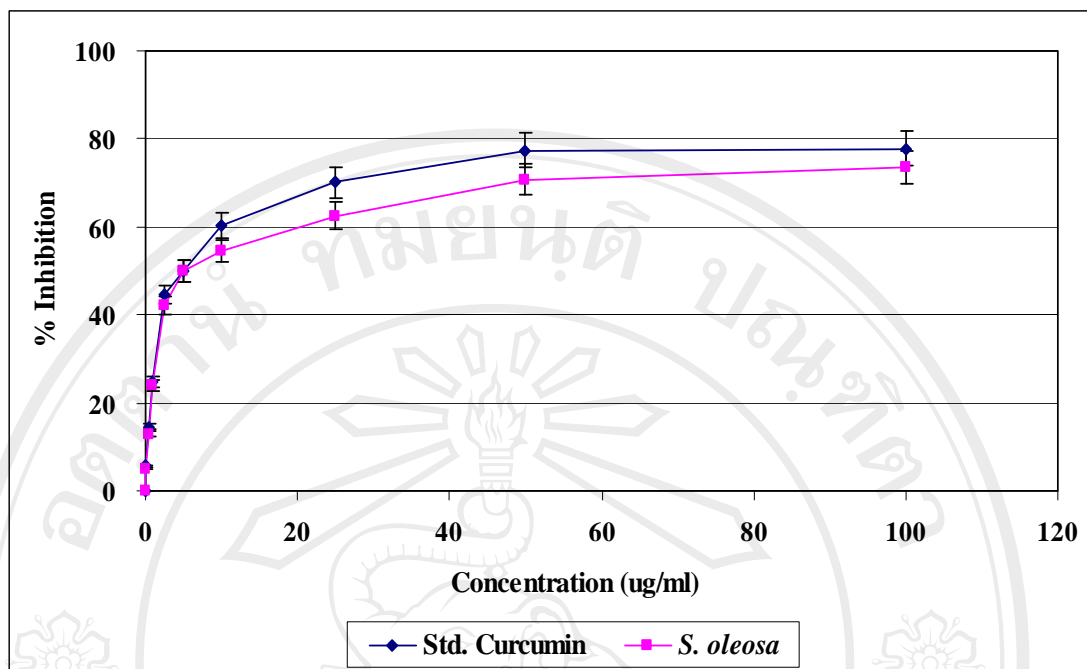


Figure 32. Dose-response curve on nitric oxide scavenging activity of *S. oleosa*

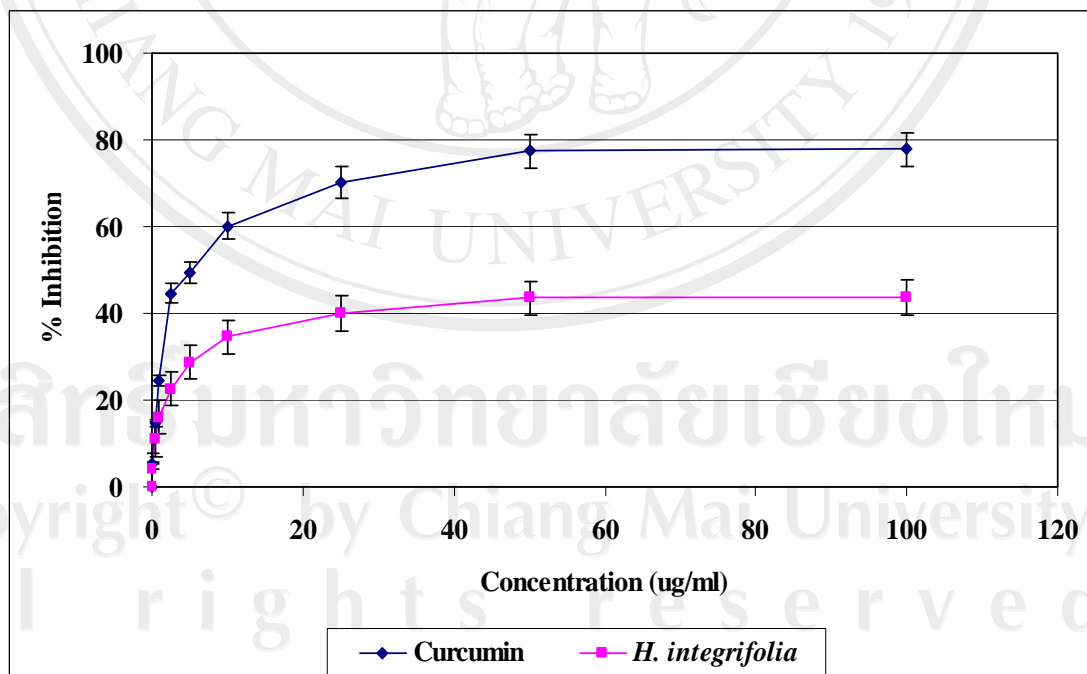


Figure 33. Dose-response Nitric oxide scavenging activity of *H. integrifolia*

Table 6. 50% Effective concentration of six medicinal plants in Northern Thailand extract on nitric oxide scavenging activity. The data are expressed as the mean \pm SD (n=3). The results are significantly difference at $P < 0.05$.

Plant extracts	Standard	Nitric oxide scavenging activity
		EC ₅₀ (μ g/ml)
<i>C. sappan</i>	-	4.24 \pm 0.14 ^a
<i>L. rubra</i>	-	5.49 \pm 0.23 ^b
<i>S. albiflorum</i>	-	4.47 \pm 0.09 ^a
<i>V. volkamerifolia</i>	-	6.08 \pm 0.19 ^c
<i>S. oleosa</i>	-	6.38 \pm 0.16 ^c
<i>H. integrifolia</i>	-	10.18 \pm 0.27 ^d
-	Curcumin	5.70 \pm 0.08 ^b

The results are shown as percent NO radical scavenging in Figure 28-33. All extracts exhibited the concentration dependent on NO radical scavenging. The EC₅₀ of each extract was calculated according to the relationship of concentration and % inhibition, which exhibited in Table 6. *C. sappan*, *S. albiflorum*, and *L. rubra* exhibited a good NO scavenging *in vitro* and the scavenging activity was better than curcumin, the reference standard used. *C. sappan*, *S. albiflorum*, and *L. rubra* had the best activity at the concentration 100 μ g/ml where 75.78, 62.37, and 73.56% NO scavenging were observed, respectively. *V. volkamerifolia*, *S. oleosa* and *H. integrifolia* exhibited the NO scavenging activity less than curcumin and the best activity at the concentration 100 μ g/ml where 35.53, 73.45 and 43.75% NO scavenging were observed.

4.4.4 Peroxynitrite scavenging activity assay

Inflammation is accompanied by an increased number of cells mediating non-specific immune response. Phagocytic white blood cells are importance in host defense and may inflict oxidative damage during inflammatory processes (Weiss, 1989). Beside the oxidation of cellular biomolecules, nitration of protein tyrosine residues is of particular interest in human pathology of inflammation. The product 3-nitrotyrosine has been identified in numerous infectious and inflammatory diseases (Ischiropoulos, 1998).

The functional consequence of protein nitration have not been fully clarified, but in some diseases 3-nitrotyroine formation may be causally linked to pathogenesis through modulation of signaling pathway (Kong, 1996), interference with enzyme function (Macmillan-Crow, 1998), or structural protein assembly (Eiserich, 1999).

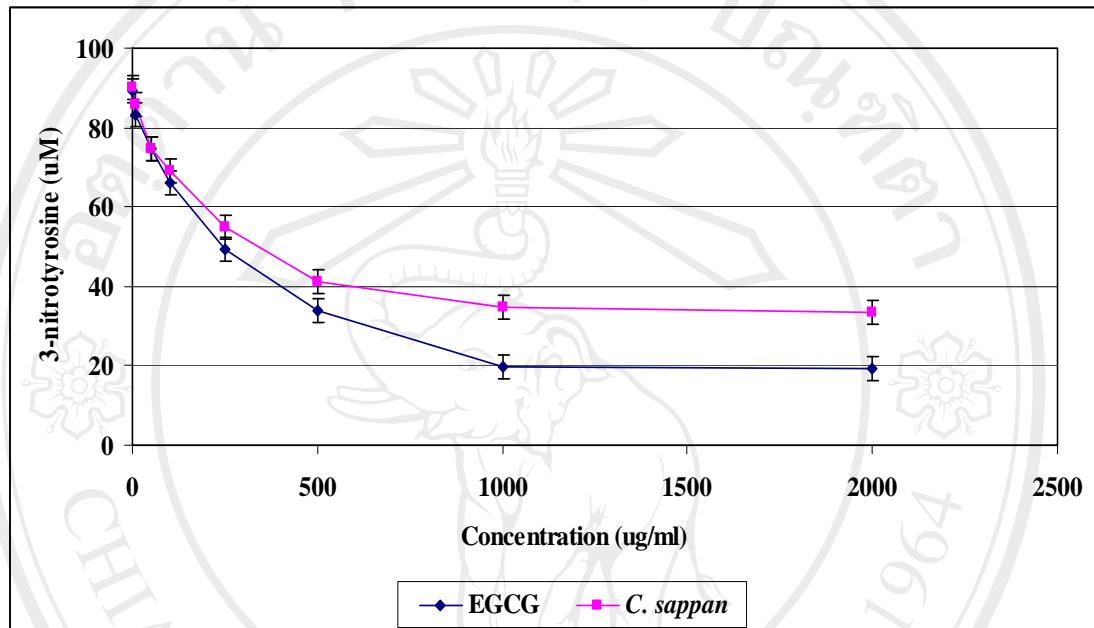


Figure 36. Effect of *C. sappan* on formation of 3-nitrotyrosine

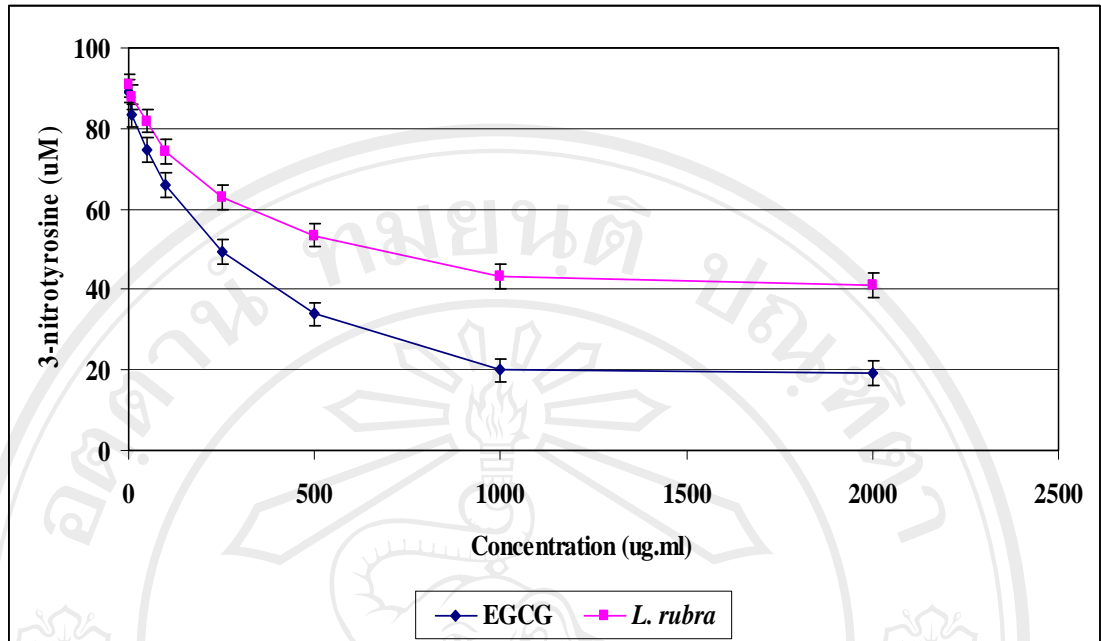


Figure 35. Effect of *L. rubra* on formation of 3-nitrotyrosine

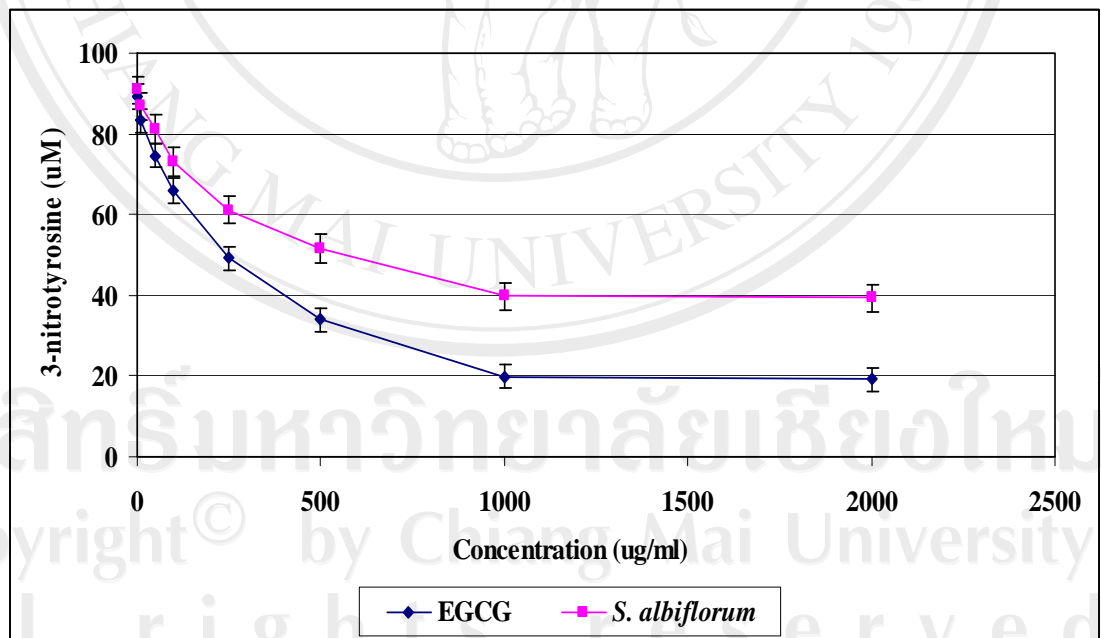


Figure 36. Effect of *S. albiflorum* on formation of 3-nitrotyrosine

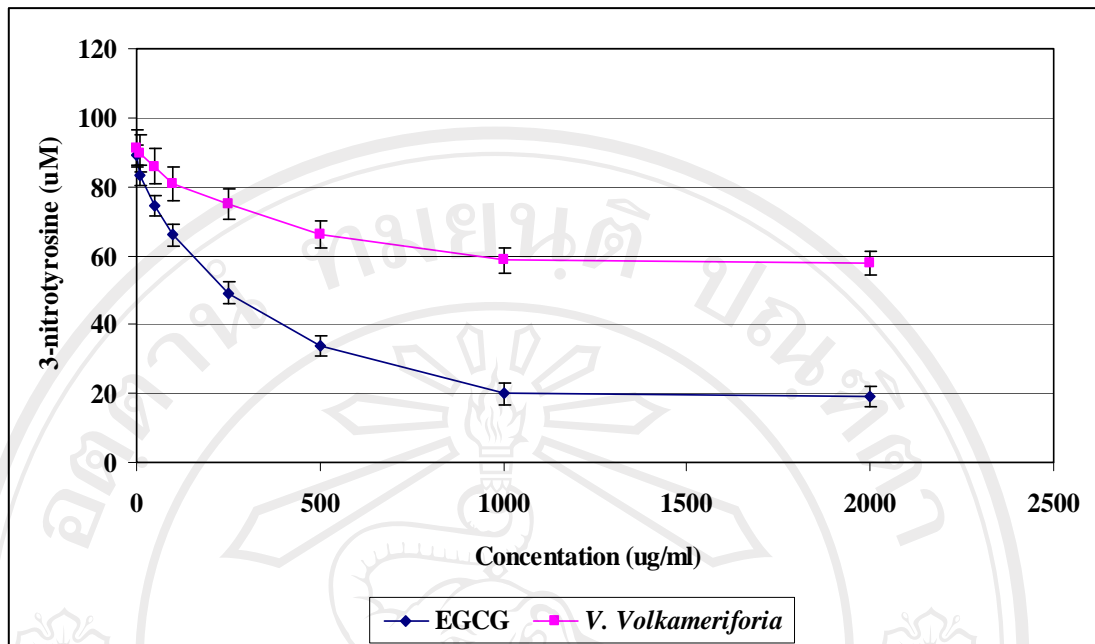


Figure 37. Effect of *V. volkameriforia* on formation of 3-nitrotyrosine

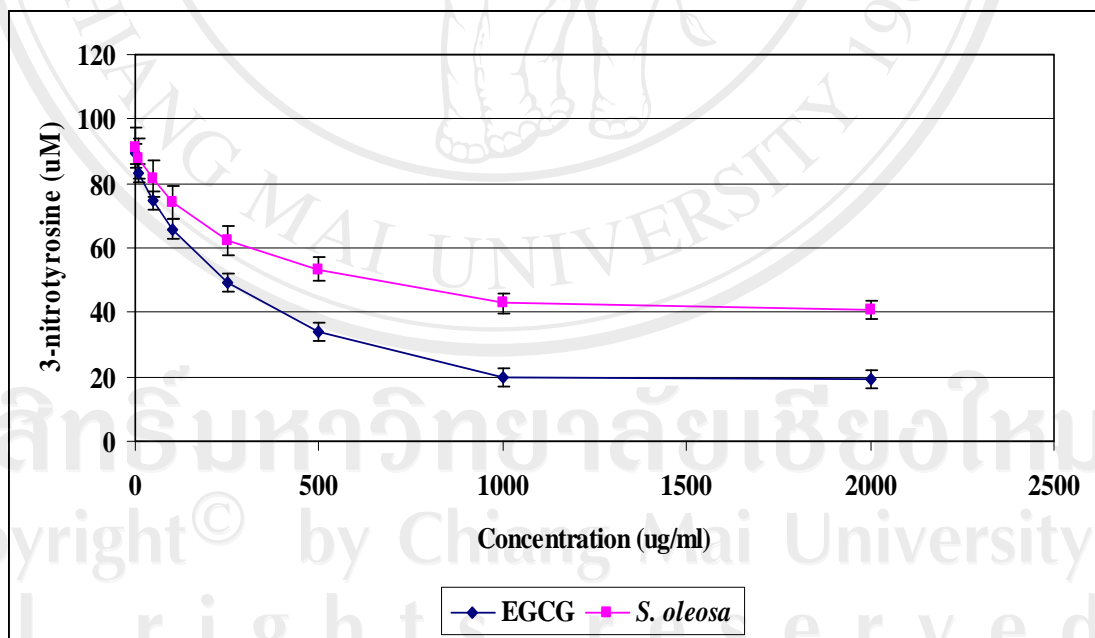


Figure 38. Effect of *S. oleosa* on formation of 3-nitrotyrosine

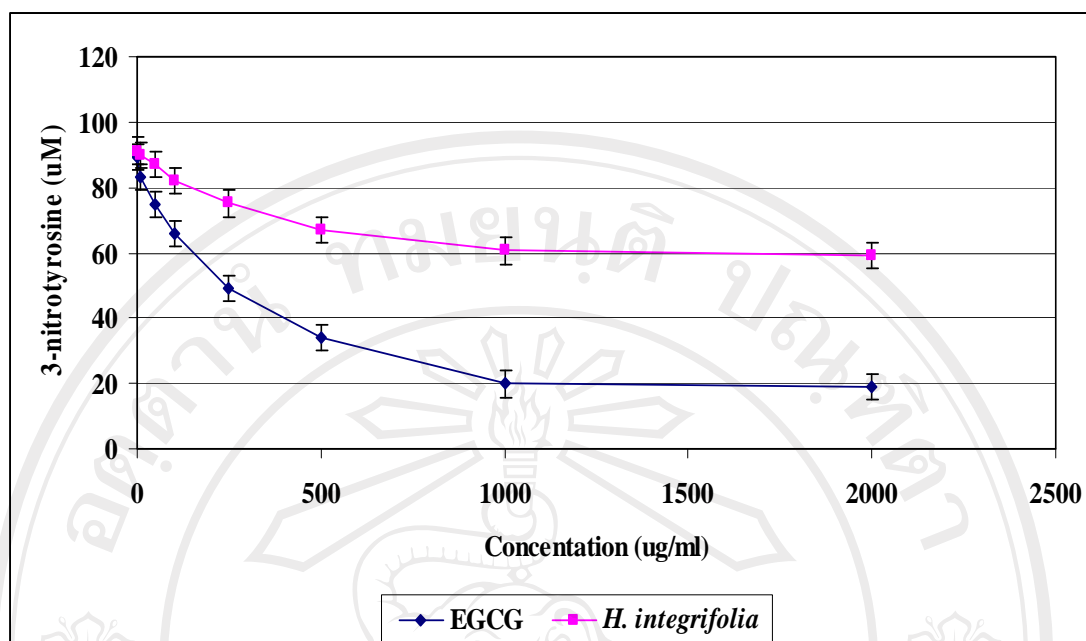


Figure 39. Effect of *H. integrifolia* on formation of 3-nitrotyrosine

Table 7. 50% Effective concentration of six medicinal plants in Northern Thailand extract on peroxynitrite scavenging activity. The data are expressed as the mean \pm SD (n=3). The results are significantly difference at $P < 0.05$.

Plant extracts	Standard	Peroxynitrite scavenging activity
		EC ₅₀ (μ g/ml)
<i>C. sappan</i>	-	178.3 \pm 2.79 ^a
<i>L. rubra</i>	-	212.0 \pm 2.50 ^c
<i>S. albiflorum</i>	-	201.4 \pm 2.57 ^b
<i>V. volkamerifolia</i>	-	235.2 \pm 4.12 ^d
<i>S. oleosa</i>	-	204.0 \pm 2.72 ^b
<i>H. integrifolia</i>	-	252.6 \pm 4.74 ^e
-	EGCG	202.7 \pm 2.17 ^b

The results are shown as peroxynitrite scavenging activity in Figure 34-39. All extracts exhibited the concentration dependent on peroxynitrite scavenging. The EC₅₀ of each extract was calculated according to the relationship of 3-nitrotyrosine concentration

and sample concentration, which exhibited in Table 7. *C. sappan* and *S. albiflorum* exhibited a high peroxynitrite scavenging *in vitro* and the scavenging activity was better than EGCG, a reference standard used. *L. rubra*, *V. volkamerifolia*, *S. oleosa*, and *H. integrifolia* exhibited the peroxynitrite scavenging activity less than EGCG.

4.4.5 Determination of DNA damage protection-induced by Fenton reaction

Plasmid DNA is occurrence as covalently closed supercoiled cyclic DNA molecules. As such it has no breaks in either strand. This supercoiled state (form I) is intrinsically less stable than uncoiled state and the breakage of a single strand instantly converts a supercoiled cyclic DNA molecule into simple relaxed cyclic state (form II). The extent of single strands breakage can follow by analyzing electrophoresis behaviour of small supercoiled DNA molecule in agarose gels. Before and after oxidant treatment, the faster migrating supercoiled form being converted to the slower moving relaxed form. A single double-strand break on the other have gives a linear DNA molecule (form III) which migrates in agarose gels at a positive intermediary between supercoiled form and relaxed form.

The role of the extract in altering the Fenton reaction induced strand break in plasmid DNA PUC18 was investigated. Fenton reaction induces many strand breaks in DNA by generation of hydroxyl radicals and subsequent free radical induced reaction on the DNA backbone. This leads to the formation of relaxed circular form of DNA and these are visualized by horizontal gel electrophoresis. Detailed analysis was carried out regarding the extent of the relaxed cyclic and the supercoiled form before and after exposed to hydroxyl radical, generated from Fenton-reaction.

In order to observe the protective effect of *C. sappan*, *L. rubra*, *S. albiflorum*, *V. volkamerifolia*, *S. oleosa*, and *H. integrifolia* against Fenton reaction-induced damage of DNA, used the Fenton reaction between Fe(II) and H₂O₂ to induce plasmid DNA PUC18 breakage. A dilution with *C. sappan* that efficient protection supercoiled DNA PUC18 damaged from Fenton reaction can be observed for a concentration of 5 µg/ml.

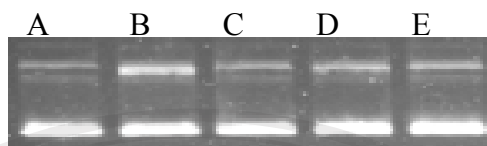


Figure 40. Electrophoresis picture of plasmid DNA PUC18. The sample was treated by 8 μ M Fe (II) and 25 mM H₂O₂ for 60 minutes with different concentrations of *C. sappan*: (A) control; (B) 1 μ g/ml; (C) 5 μ g/ml; (D) 25 μ g/ml; and (E) 50 μ g/ml.

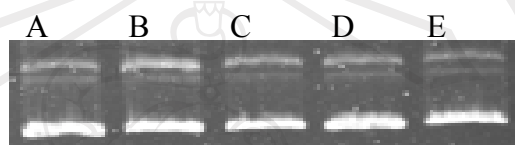


Figure 41. Electrophoresis picture of plasmid DNA PUC18. The sample was treated by 8 μ M Fe(II) and 25 mM H₂O₂ for 60 minutes with different concentrations of *L. rubra*: (A) control; (B) 1 μ g/ml; (C) 5 μ g/ml; (D) 25 μ g/ml; and (E) 50 μ g/ml.

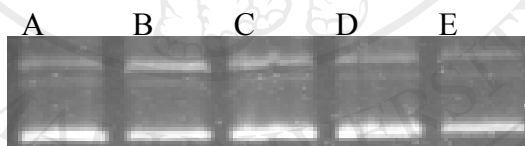


Figure 42. Electrophoresis picture of plasmid DNA PUC18. The sample was treated by 8 μ M Fe(II) and 25 mM H₂O₂ for 60 minutes with different concentrations of *S. albiflorum*: (A) control; (B) 1 μ g/ml; (C) 5 μ g/ml; (D) 25 μ g/ml; and (E) 50 μ g/ml.

The dilution with *L. rubra* and *S. albiflorum* that efficient protection supercoiled DNA PUC18 damaged from Fenton reaction can be observed for a concentration of 25 and 25 μ g/ml, respectively. *V. volkameriforia* can not protection supercoiled DNA PUC18 damaged from Fenton reaction at the maximum concentration of 50 μ g/ml.

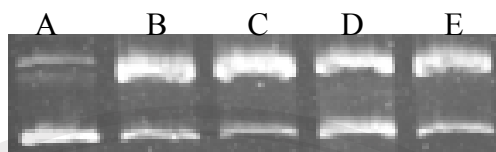


Figure 43. Electrophoresis picture of plasmid DNA PUC18. The sample was treated by 8 μM Fe(II) and 25 mM H_2O_2 for 60 minutes with different concentrations of *V. volkamerifolia*: (A) control; (B) 1 $\mu\text{g/ml}$; (C) 5 $\mu\text{g/ml}$; (D) 25 $\mu\text{g/ml}$; and (E) 50 $\mu\text{g/ml}$.

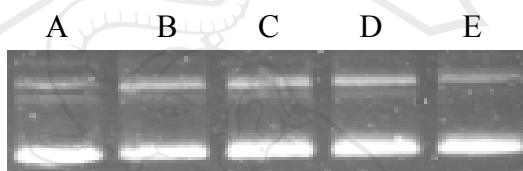


Figure 44. Electrophoresis picture of plasmid DNA PUC18. The sample was treated by 8 μM Fe(II) and 25 mM H_2O_2 for 60 minutes with different concentrations of *S. oleosa*: (A) control; (B) 1 $\mu\text{g/ml}$; (C) 5 $\mu\text{g/ml}$; (D) 25 $\mu\text{g/ml}$; and (E) 50 $\mu\text{g/ml}$.

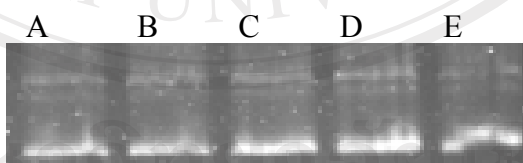


Figure 45. Electrophoresis picture of plasmid DNA PUC18. The sample was treated by 8 μM Fe(II) and 25 mM H_2O_2 for 60 minutes with different concentrations of *H. integrifolia*: (A) control; (B) 1 $\mu\text{g/ml}$; (C) 5 $\mu\text{g/ml}$; (D) 25 $\mu\text{g/ml}$; and (E) 50 $\mu\text{g/ml}$.

The dilution with *S. oleosa* that efficient protection supercoiled DNA PUC18 damaged from Fenton reaction can be observed for a concentration of 50 $\mu\text{g/ml}$. *H. integrifolia* can not protection supercoiled DNA PUC18 damaged from Fenton reaction at the maximum concentration of 50 $\mu\text{g/ml}$.

4.5 Determination of total phenolic compounds

Phenolic compounds are the principal antioxidant constituents of natural products and are composed of phenolic acids and flavonoids, which are potent radical terminators (Shahidi, 1992). They donate hydrogen to radicals and break the reaction of lipid peroxidation at the initial step (Gulcin, 2004). The high potential of polyphenols to scavenge free radicals may be because of their many phenolic hydroxyl groups (Sawa, 1999). The total polyphenol content of sample extracts were determined by the Folin-Denis colorimetric method. This method is based on the reduction of Folin-Denis reagent by the electrons from the phenols. The absorbance was measured at 725 nm by using UV/VIS spectrophotometer.

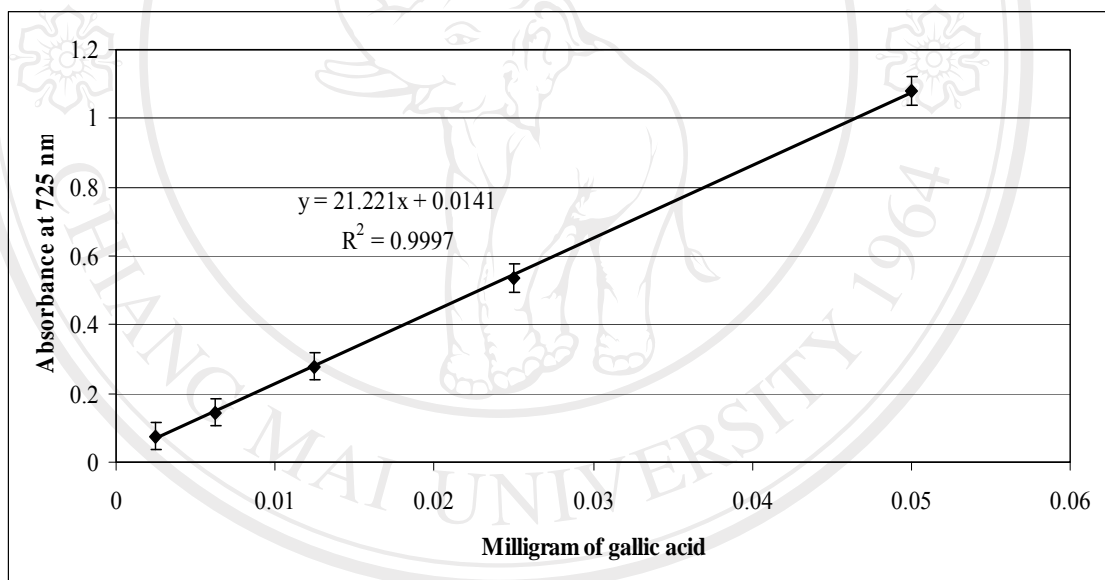


Figure 46. Calibration curve of Folin-Denis assay using gallic acid as standard

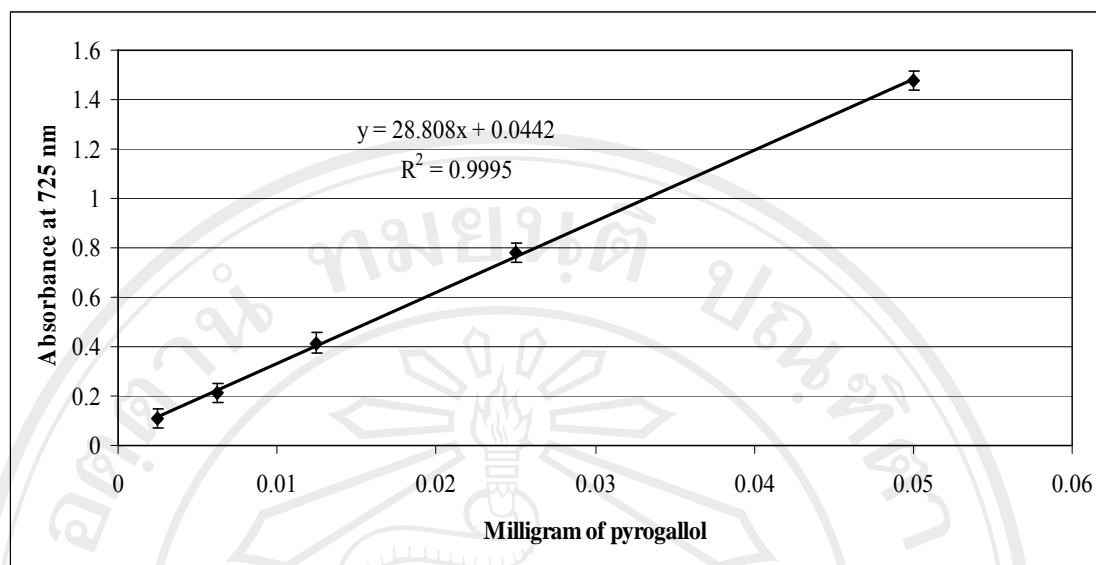


Figure 47. Calibration curve of Folin-Denis assay using pyrogallol as standard

Gallic acid and pyrogallol were used as standards. Standard curves were shown in Figure 46 and 47, respectively. Total polyphenol content was expressed as milligram equivalents of gallic acid or pyrogallol per milligram of sample extract. Based on the absorbance values of the various extract solutions, reacted with Folin-Denis reagent and compared with the standard solutions of gallic acid and pyrogallol, results of the colorimetric analysis of total phenolic compounds are given in Table 8.

Table 8. Total phenolic compounds content of six medicinal plants in Northern Thai extract extract. The data are expressed as the mean \pm SD (n=3). The results are significantly difference at $P < 0.05$.

Plant extracts	Total phenolic compounds	
	mg gallic acid/ mg extract	mg pyrogallol/ mg extract
<i>C. sappan</i>	0.5540 \pm 0.0192 ^a	0.3947 \pm 0.0046 ^a
<i>L. rubra</i>	0.4563 \pm 0.0072 ^b	0.3225 \pm 0.0068 ^b
<i>S. albiflorum</i>	0.4048 \pm 0.0047 ^c	0.2842 \pm 0.0056 ^c
<i>V. volkamerifolia</i>	0.1205 \pm 0.0035 ^e	0.0864 \pm 0.0039 ^e
<i>S. oleosa</i>	0.3809 \pm 0.0064 ^d	0.2386 \pm 0.0031 ^d
<i>H. integrifolia</i>	0.0245 \pm 0.0012 ^e	0.0067 \pm 0.0007 ^e

The amount of total phenolic compound content was highest in *C. Sappan*, followed by *L. rubra*, *S. albiflorum*, *S. oleosa*, *V. volkamerifolia* and *H. integrifolia*, respectively. It is extremely important to point out that there is a positive correlation between antioxidant activity and amount of phenolic compounds of the extracts.

It is well-known that plant phenolics, in general, are highly effective free radical scavengers and antioxidants. Consequently the antioxidant activities of plant/herb extracts are often explained with respect to their total phenolic compounds and flavonoids contents, with good correlation. In this study also observed similar correlation between the ABTS^{•+} scavenging activity, superoxide anion scavenging activity, nitric oxide scavenging activity, peroxynitrite scavenging activity, and determination of DNA damage protection-induced by Fenton reaction. The total phenolic compounds in the extracts were determined spectrophotometrically by the Folin-Denis method. Overall, the order of the phenolic compounds content of the test samples was *C. Sappan* > *L. rubra* > *S. albiflorum* > *S. oleosa* > *V. volkamerifolia* > *H. integrifolia*, which was broadly similar to their ABTS^{•+} scavenging activity, superoxide anion scavenging activity, nitric oxide scavenging activity, peroxynitrite scavenging activity, and DNA damage protection-induced by Fenton reaction. Thus, *C. sappan* contains high levels of total phenolic compounds, which may account for its impressive antioxidant activity.

Free radicals have been implicated in inflammation condition, the important ones being superoxide anion radical, nitric oxide radical, and peroxynitrite radical. Medicinal plants in northern Thailand containing radical scavengers are gaining importance in treating this symptom. As the results of antioxidative activity, three extracts *C. sappan*, *L. rubra*, and *S. albiflorum* were chosen to determination of COX-2 inhibition activity and DNA damage protection-induced by Fenton reaction.

4.6 Determination of cyclooxygenase-2 inhibition activity

Three kinds of Northern Thai medicinal plant extracts were chosen base on the results of antioxidative activities. The extracts were evaluated COX-2 inhibition by measurement of prostaglandin produced from mouse COX-2 null cell line. In this study, the extracts were evaluated by Bioassay Laboratory, National Center for Genetic Engineering and Biotechnology (BIOTECH). Aspirin was used as a positive control with

IC₅₀ value at 0.9 – 1.0 x 10⁻² mg/ml. The extracts did not have COX-2 inhibition activity at the maximum final concentration of tested sample 10⁻² mg/ml.

Hong, C.H. et al. were evaluated of 170 methanol extracts of natural products on inhibition of iCOX-2 and iNOS in cultured mouse macrophage RAW264.7 cells. As a result, several extracts such as *Aristolochia debilis*, *Cinnamomum cassia*, *Curcuma zedoaria*, *Eugenia caryophyllata*, *Pterocarpus santalius*, *Rehmania glutinosa* and *Tribulus terrestris* showed potent inhibition of COX-2 activity (>80% inhibition at the test concentration of 10 µg/ml), the activity was comparable to celecoxib with 98.2% inhibition at 10 µg/ml. In addition, the extract of *A. debilis*, *C. sappan*, *Curcuma longa*, *C. zedoaria*, *Daphne genkwa* and *Moreus alba* were also considered as potential inhibitors of iNOS activity (>70% inhibition at the test concentration of 10 µg/ml), the activity was comparable to L-N^G-monomethyl arginine (L-NMMA) with the 69.2% inhibition at 10 µg/ml. *C. sappan* exhibited potent inhibition iNOS activity with 71.0% inhibition at the concentration of 10 µg/ml and weak activity on COX-2 inhibition with the 40.1% inhibition at the concentration of 10 µg/ml.